WATER DROPLET ACCUMULATION AND MOTION IN PEM FUEL CELL MINI-CHANNELS

J. G. Carton[1*], V. Lawlor[1, 2], A. G. Olabi[1], C. Hochenauer[2], G. Zauner[2]

1. Department of Manufacturing and Mechanical Engineering, Dublin City University, Dublin 9, (Ireland).
2. School of Engineering and Environmental Sciences, Upper Austria University of Applied Science, A-4600 Wels, (Austria).

*Email: James.carton3@mail.dcu.ie Phone: +353876328459

ABSTRACT

Effective water management is one of the key strategies for improving low temperature Proton Exchange Membrane (PEM) fuel cell performance and durability. Phenomena such as membrane dehydration, catalyst layer flooding, mass transport and fluid flow regimes can be affected by the interaction, distribution and movement of water in flow plate channels.

In this paper a literature review is completed in relation to PEM fuel cell water flooding. It is clear that droplet formation, movement and interaction with the Gas Diffusion Layer (GDL) have been studied extensively. However slug formation and droplet accumulation in the flow channels has not been analysed in detail. In this study, a Computational Fluid Dynamic (CFD) model and Volume of Fluid (VOF) method is used to simulate water droplet movement and slug formation in PEM fuel cell mini-channels. In addition, water slug visualisation is recorded in ex situ PEM fuel cell mini-channels. Observation and simulation results are discussed with relation to slug formation and the implications to PEM fuel cell performance.

KEYWORDS: PEM Fuel Cell, Mini-channel, Flow Plate, Water flooding, Visualisation, VOF.

1 INTRODUCTION

Fuel cells produce electricity from a re-dox reaction of the fuel, hydrogen, with oxygen from the air. Fuel cells have the advantage of only producing water and heat as by products and are extremely efficient [1]. The PEM fuel cell is a low temperature electrochemical device that offers a promising, possibly green, alternative to traditional power sources and other fuel cell types in many applications without air polluting issues [2-5]. At present some barriers still persist that are hampering PEM fuel

cell system commercialisation. One of these barriers is water flooding, hindering the advance of PEM fuel cells, especially at low temperature operation [6].

1.1 Water Flooding

At high current densities liquid water accumulates at the cathode. This is as a result of the Oxygen Reduction Reaction (ORR), remembering that the electrochemical result of combining hydrogen and oxygen at a temperature below 100°C forms liquid water. Water can also be transported from the anode to the cathode, through the membrane, via electro-osmotic drag and local pressure, temperature and concentration gradients [7]. If a nafion membrane is used, it must be fully hydrated for it to be a good proton conductor. In order to maintain the membrane hydration level, especially at start up; the reactant and oxide gases are often fully humidified with water. When a PEM fuel cell accumulates too much water at high current density, about one-third of the electrode surface area may not be utilised [8, 9]. The phenomenon of flooding is a well established problem at the cathode electrode where both the catalyst layer and/or the Gas Diffusion Layer (GDL) may be mass transport-limited due to condensed water [10, 11]. This water flooding increases the internal resistance of the cell, blocks the ORR reaction, disrupts cell pressure and gas flow, making the cell voltage and current unpredictable and unrepeatable, reducing the PEM fuel cell performance dramatically. Many factors affect how water is transported from the catalyst layer to the flow plate and how droplet formation occurs, grows and ultimately how water flooding occurs within the PEM fuel cell flow channels. These factors include the membrane, flow plate or flow field channel design, air flow rate, temperature, power density, gas humidification as well as PEM fuel cell orientation.

If the cathode layer or GDL floods, water must be transported from the electrode, through the GDL and into the flow plate flow channels and then exhausted out of the cell to mitigate the flooding problems. The water transport mechanism from the GDL into the flow plate channels has been explained by two theories; converging capillary tree water transport mechanism proposed by Nam and Kaviany [12] and channelling liquid water transport mechanism proposed by Litster et al. [13]. There are discrepancies between both theories; however, both theories concur that water droplets can form on the GDL and that these droplets, mainly originate from the electro-catalyst layer. These droplets

join and grow in the GDL and squeeze out into the channels due to capillary action within the GDL, its hydrophobic nature and due to pressure and temperature forces in the flow plate channels [14-17].

Many researchers have observed and modelled water droplet formation and emergence from GDL pores [18, 19]. Kimball et al. [22] measured the critical hydrostatic pressure head for liquid water breakthrough for various GDL materials. Kumbur et al. [20] employed an ex situ flow channel apparatus in order to study droplet formation and instability. Park et al. [21] modelled fluid flow through GDLs where it was concluded that a thin GDL with small porosity results in good electrical conductivity; however efficient mass transport requires large pores. Many authors including, Yang et al. [23], Hakenjos et al. [24] and Gao et al. [25] describe preferential location emergence of droplets from the GDL relating it to temperature distribution or capillary action within the GDL. Zhu et al. [26] modelled liquid water entering a PEM fuel cell channel through a GDL pore. A 2-D VOF model was employed to view the effects of flow channel size, droplet coalescence and pore size on the emerging water droplet dynamics. It was found that in large micro-channels (0.5mm) droplet deformation slows down and droplet breakup may not occur. This can result in a film of water forming against the GDL downstream of the pore. Researchers have also produced water flooding mitigation methods and models. Tüber et al. [27] visualised liquid water transport in the cathode gas channel of a transparent PEM fuel cell at low operating temperatures (30°C). They found that using a hydrophilic cathode GDL resulted in increased current density, which they attributed to a more uniformly hydrated membrane. This was also noted by Ge and Wang [28] who visualized water droplet formation in the anode flow channels. They observed that droplets tended to form on the gas channel walls when a hydrophobic GDL was employed, whereas a hydrophilic GDL tended to wick water from the channel into the GDL. Quan et al. [29] also studied the water management in a PEM fuel cell flow channel. This study focused on the effects of channel hydrophilicity, channel geometry, air inlet velocity and pressure drop in relation to water behaviour. It was concluded that sharp corners inside the channel with the aid of hydrophilic surfaces may aid in water transport and due to increased spreading of the liquid, pressure drop is increased in the flow channel. Liu et al. [30] investigated the

liquid water accumulation in PEM fuel cells cathode flow channels with three different flow field configurations: parallel, interdigitated, and cascaded. At low operating temperatures (25°C) and ambient pressure, they observed that the parallel flow field was the most unsuitable flow field design for water removal, resulting in the worst performance of the PEM fuel cell. In a study by Zhu et al. [31], the effect of micro-channel geometry on water droplet dynamics in a PEM fuel cell using a 3-D VOF model, was investigated. They compared many different micro-channel designs; rectangular, trapezoid, upside down trapezoid, triangular, rectangular with curved bottom wall and semicircular with respect to evolution and motion of the droplets, flow resistance, saturation and coverage ratio. They concluded that the geometry and the micro-channels wet-ability drastically affect water droplet movement which should help design better flow channels for more effective water removal. Carton and Olabi [32] performed a Design of Experiment (DOE) study on three PEM fuel cell flow plate configurations. It was concluded that over all the serpentine flow plate performed best, due to its continuous flow design water flooding was mitigated. Li et al. [33] also concluded that the serpentine plates offer the best results for water removal, since it ensures the removal of water produced from a cell with acceptable parasitic load. Ous and Arcoumanis [34] noted that increased airflow rate prevented droplet formation but reduced current due to membrane dehydration. Again, Weng et al. [35] confirmed the beneficial effects of high cathode gas flow rates for water removal; however un-humidified cathode gas streams at high stoichiometry resulted in membrane dehydration.

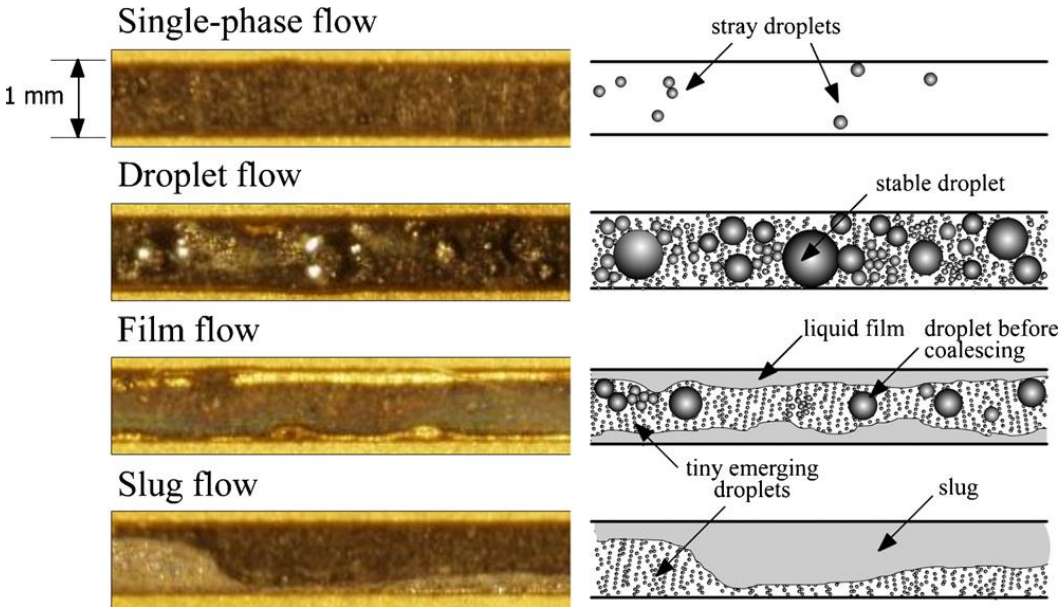

Contact: James.Carton3@mail.dcu.ie

Figure 1 Water transport through channels of an operational PEM fuel cell [36]**.**

Overall, however, only a few researchers have investigated slug movement in flow channels and this area has not been analysed to the same degree as droplet formation and emergence from GDL pores. Hussaini et al. [36] presented images corresponding to the most common flow patterns in operational PEM fuel cells. These include; single phase flow, droplet flow, film flow and slug flow as shown in Figure 1. The authors explain that these flows can evolve from each other resulting in slug flow, which was a consequence of film flow growth. Lu et al. [37] also observed three different types of water to air flow regimes in their study, slug flow, annular/film flow and mist flow. They noted that slug flow and intense annular flow cause an increased pressure drop due to liquid water build-up, which is a key cause of flow misdistribution that dramatically reduces the PEM fuel cell performance and durability.

Zhau et al. [38] studied water behaviour in the cathode side of a PEM fuel cell, with a serpentine channel using VOF. Water droplets and films were introduced into the channel at varying positions, to simulate different operational conditions of the PEM fuel cell and high air flow rates ($10ms^{-1}$) were used. Detailed results show droplet evolution, breakup and movement of water films through the serpentine micro-channel. However, Ous and Arcoumanis [34] viewed the formation of water droplets emerging from an operational PEM fuel cell (Figure 2). A transparent proton exchange membrane fuel cell was used to visualise the water droplet formation during its operation. Visualisation results show that water accumulates first in the middle flow channels and that no accumulation takes place at the bend areas. Droplets were observed to appear and then shrink on the GDL, which they attributed to their increased cross-sectional area in the direction of the airflow, which may push the droplet back into the GDL. The droplets grew larger and then adhered to the channel walls. It is shown that after 95 minutes of operation droplets can join to fill the channel, as shown in Figure 2. Measurement of the fuel cell current during water production showed that the current gradually declined as more water filled the channel.

Contact: James.Carton3@mail.dcu.ie

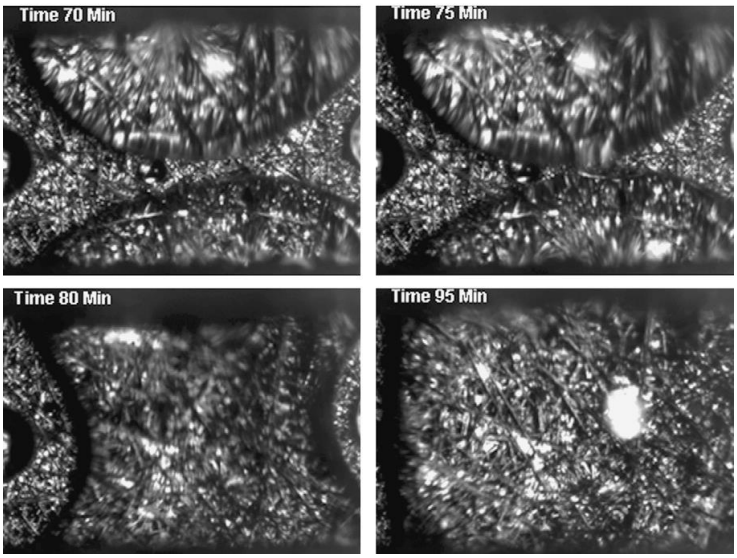

Figure 2 Formation of water droplets emerging from an operational PEM fuel cell [34]**.**

Water flooding analysis, in literature, has mainly focused on droplet and micro-droplet release from the GDL and their interaction within the flow field channels. However, to design effective flow channels and to aid the mitigation of water flooding, water droplets after their emergence from the GDL and consequential interaction with each other and the flow channels must be investigated and analysed. It has also been shown from literature that water, from the GDL, has preferential location emergence and does not emerge in a film form, but discrete droplets on the GDL, if a hydrophobic GDL is used. These droplets can then join to form a slug. The definition of a slug in this study is a large water droplet that adheres to either the GDL or channel wall and moves in air flow. In this study, a two-phase flow model is developed, viewing three different scenarios, where the coalescence of droplets and movement of water slugs in flow field mini-channels are investigated. To simplify the model water droplets are introduced into the channel inlet. This model, however, can represent any region of the flow plate where slugs may occur. In addition with the aid of imaging techniques, visualisation of water droplets and slugs are recorded in ex situ flow channels to ensure valid results from the model. The implication of slugging on flow plate design and PEM fuel cell performance is discussed.

2 VOLUME OF FLUID MODEL

In the present study suitable Computational Fluid Dynamic (CFD) software using Volume of Fluid (VOF) was applied in order to simulate fluid motion in mini-channels without heat transfer. VOF is a

surface-tracking technique applied to a fixed Eulerian mesh. It is designed for two or more immiscible fluids, where the position of the interface between the fluids is of interest. In the VOF model, a single set of momentum equations are shared by the fluids, and the volume fraction of each of the fluids in each computational cell is tracked throughout the domain. Applications of the VOF model include stratified flows, free-surface flows, slug flows, filling, sloshing, the motion of large bubbles in a liquid, the motion of liquid after a dam break, the prediction of jet breakup (surface tension), and the steady or transient tracking of any liquid-gas interface [39].

Annaland et al. [40] used VOF to create a model that would accurately represent gas bubbles rising in liquids. The results matched results from the Grace Bubble diagram. Lai et al. [41] used VOF to study thermo-capillary induced flow in a micro-channel. Using drops of water in micro-channels a capillary pressure gradient for liquid propulsion was generated by applying a difference in temperature between the front and back ends of the micro-channel. Theodorakakos et al. [42] utilized a flow field to capture side-view droplet detachment images for input to their VOF simulations and again the model matched well with experiment. From literature it is concluded, that VOF has proven suitability for droplet simulation and model and experimental result should match well.

A double serpentine flow field was chosen for the simulation and experimental investigations. The serpentine flow field is a common flow channel and reported on well in literature. The advantage of this flow field is that it investigates the straight portion of the mini-channel ($1mm^2$) and the bend region of a mini-channel. In addition, having parallel channels, this flow plate configuration will show if a problem in one channel can affect the adjacent parallel channel. The double serpentine flow field model is shown in Figure 3.

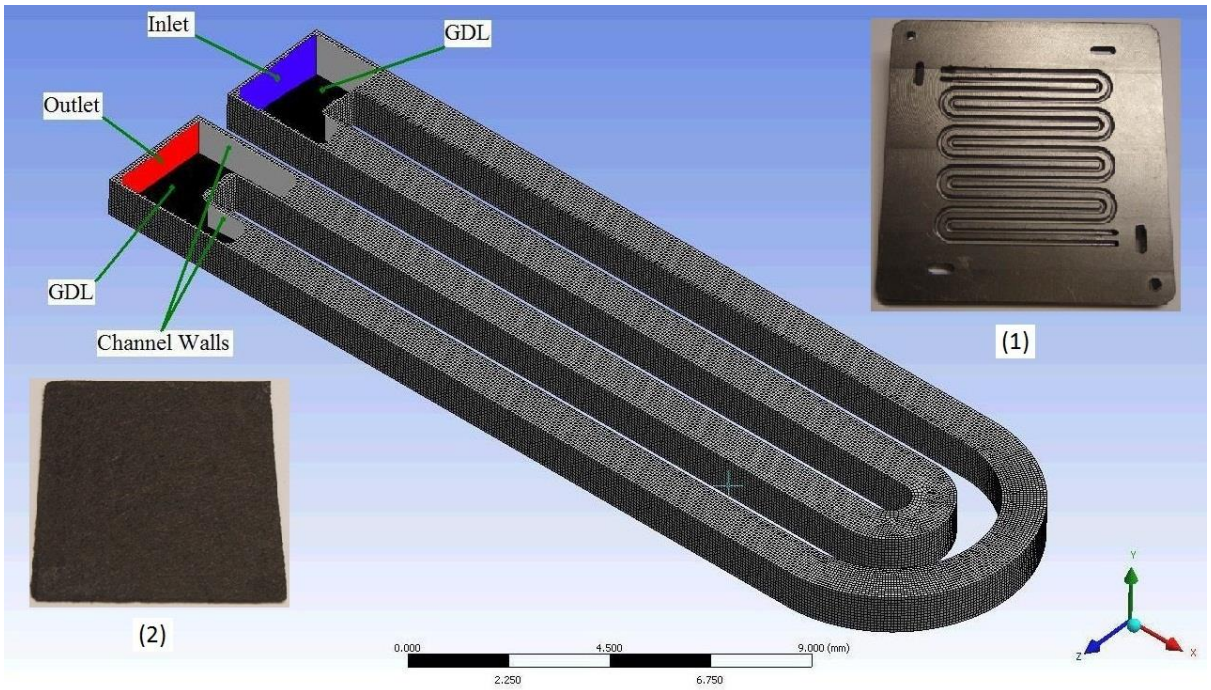

Figure 3 3-D double serpentine model, inset (1) actual serpentine flow plate (2) actual carbon paper GDL used in the PEM fuel cell.

The computation domain consists of a double serpentine flow channel with inlet and outlet. The boundary wall is divided in to two sections; the GDL and mini-channel walls. For the current model the GDL and flow channel walls are specified as solid, shear condition (no slip) and contact angle (hydrophobic or hydrophilic), refer to Table 1. The mini-channel side and top walls are specified hydrophilic, due to the nature of the flow channel material. The floor of the double serpentine mini-channel represents the GDL which is specified to be hydrophobic, due to the presence of PTFE in the GDL material. The CFD software allows the walls of the model to be specified as a specific solid material. The flow channel is specified as graphite and the GDL as carbon paper. The properties of these materials were detailed as per the manufacturer of the fuel cell components (H_2ECOnomy). The PEM fuel cell flow plate and GDL are shown in Figure 3, inset (1) and (2) respectively.

The domain is patched with a drop or slug of water, volume fraction one. Each drop or slug was placed between 3mm and 5mm from the inlet and each had a diameter of between 0.3mm and 0.9mm. The model represents an operational PEM fuel cell flow field after approximately 60 to 80 minutes of fuel cell operation (according to Ous and Arcoumanis [34]). Please refer to Table 1 for CFD settings and boundary conditions. The total number of cells used in the complete double serpentine model was

about 268,000 and each model took about five hours to complete. The model converged in fewer than 100 iterations. Grid independence was completed by testing each case with at least three different types of grids and analysing the CFD model predictions. It was found that a hexahedral conformal grid consisting of about 260,000 cells enabled predictions that sufficiently matched grids with much more cells. The aspect ratio, equisized skew and the largest volume change were all within general accepted limits and are thus indications of high quality grids.

Table 1 Model boundary conditions.

Multiphase model	VOF
Model design	Double serpentine
Computation grid	20 x 1 x 1 mm
Grid size	0.0025mm^2
Scheme	Explicit
Phase 1	Air
Phase 2	Water
Solver type	Pressure – based
Time	Transient
Temperature (constant)	328K
Gas phase	Ideal mixture
Fluid flow	Laminar
Gravity	0
Number of time steps	1520
Time step	0.00001 sec
Drop radius	0.3 – 0.9 mm
Initial drop position	(x, y, z) = (2, 0.1, 0.5)
Inlet velocity	1 ms^{-1}
Outlet pressure	0 Bar (Gauge)
Wall wet	90
Wall not wet	150
Interface representation	PLIC
Surface tension	0.073Nm

3 EXPERIMENTAL SETUP

A detailed review of liquid water visualisation in PEM fuel cells was recently conducted by Bazylak [43]. Many liquid water visualisation techniques including nuclear magnetic resonance (NMR), beam interrogation and direct optical imaging techniques were mentioned. The reviewer concluded that even with the difficulties posed by direct optical imaging such as opaque materials or in/ex situ apparatus and limitations of magnification and speed of the camera used, direct optical visualisation

(used in the current study) of liquid water in PEM fuel cell flow channels can provide high temporal and spatial resolution information and can be easier and cheaper to implement than other techniques.

The experimental setup is shown diagrammatically in Figure 4 and pictorially in Figure 5. An air compressor supplies air to an air reservoir, with the output pressure controlled by a pressure regulator (SMC). The air then passes through a volumetric flow meter (Voegtlin red-y series flow controller). The flow controller was calibrated for air. The flow controller is controlled by the data acquisition (DAQ) software (Lab View).

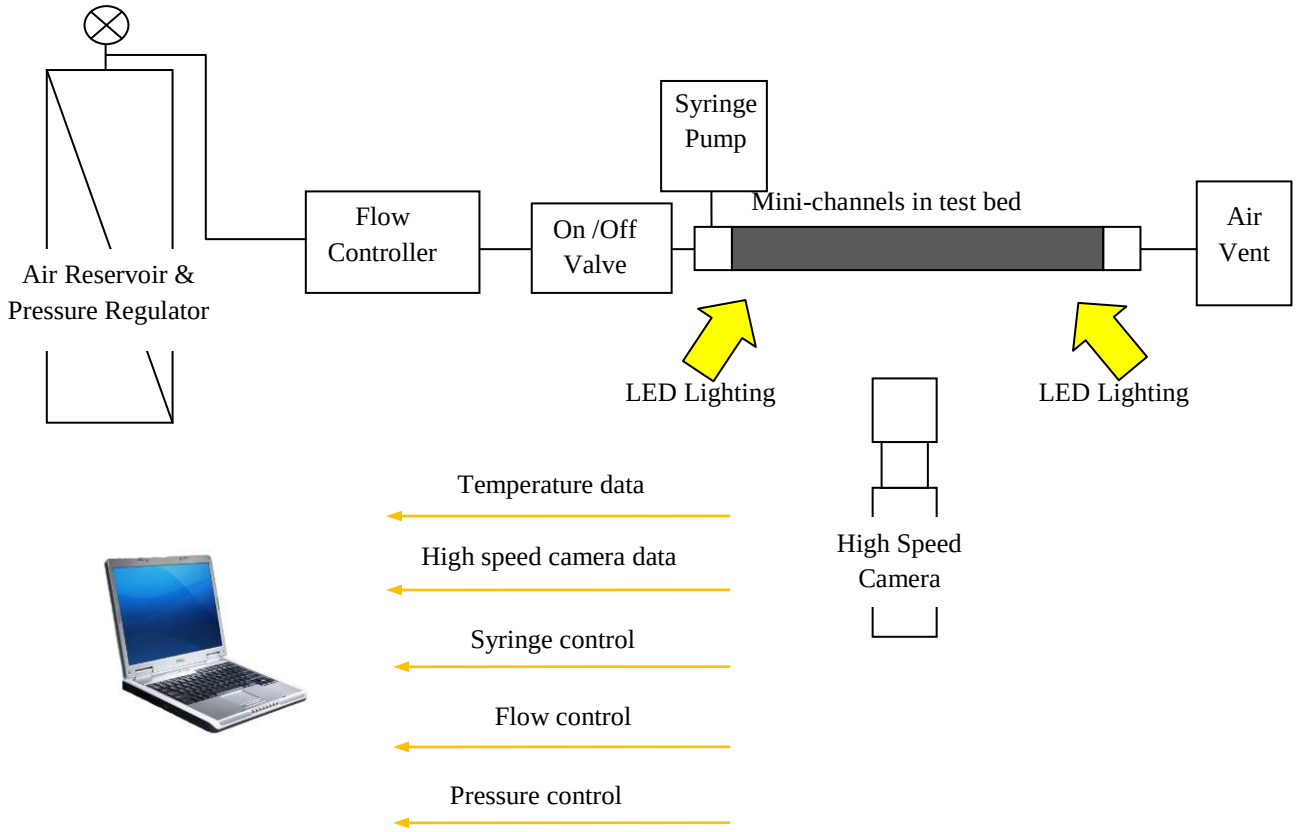

Figure 4 Diagram of experimental apparatus to investigate water slug and droplet flow regimes in ex situ PEM fuel cell channels.

A strip heater was used to heat the apparatus. A thermocouple was placed into the test bed and the temperature value was recorded through the DAQ system. The location of the thermocouple in the test bed indicated that the flow channel was between 50°C and 60°C for all experiments. This was chosen to be a steady state region and fluctuations were minimised. A syringe pump (Harvard) was used to position drops of water in to the mini-channel with a tip diameter of 0.01mm. A clear polycarbonate cover was placed over the channel for visualisation purposes. Two high speed cameras (HSC), a

Citius HSC with 340 x 60 pixels at 1200 frames per second (fps) and a Mikrotron HSC with 1024 x 1024 pixels at 2000 fps, were used to capture images and high power LEDs were used to illuminate the test bed.

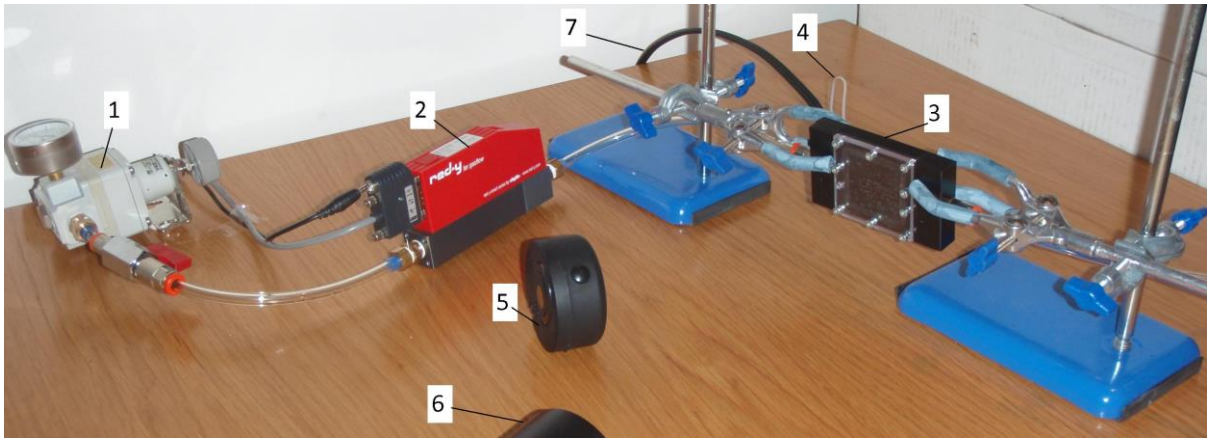

Figure 5 Experimental apparatus: (1) Pressure regulator (2) Flow controller (3) Test bed (4) Inlet for syringe pump (5) Light source (6) High speed camera (7) Thermocouple & heater cables.

3.1 Experimental Procedure

The LEDs and air are turned on. The inlet air pressure is set to 2 Bar. The flow controller is set to 50mlmin^{-1} (approximately 1ms^{-1}). The camera recording is started and the air valve is set on. A drop or slug of water is placed into the channel at least 5mm from the inlet. The recording is terminated after the experiment is completed. All information is fed back to a computer for post processing.

4 RESULTS

4.1 Model Validation

A time sequenced VOF model was simulated to view a slug movement around the double serpentine channel bends, as shown in Figure 6 (a). To ensure that the model matched reality, an experiment was performed to view slug movement around the bend of a double serpentine channel Figure 6 (b). The model and experiment shows three time instances of the slug movement as shown in Figure 6. As the slug is pushed with the air it begins to deform Figure 6 (1). Depending on the surface treatment of the channel and or the GDL, the slug leaves a trail of water behind it, particular evident at the edges of the channels in both the simulation and experiment Figure 6 (a) & Figure 6 (b). When the slug approaches the bend it continues forward until it hits the back of the channel bend, Figure 6 (2). Air begins to escape from around the slug, pushing it against the channel wall. This continues until the air escapes

leaving a layer of water towards the bottom of the channel as shown in both the model and experiment results Figure 6 (3). From this comparison the model and experiment results match well and further simulation analysis proceeded.

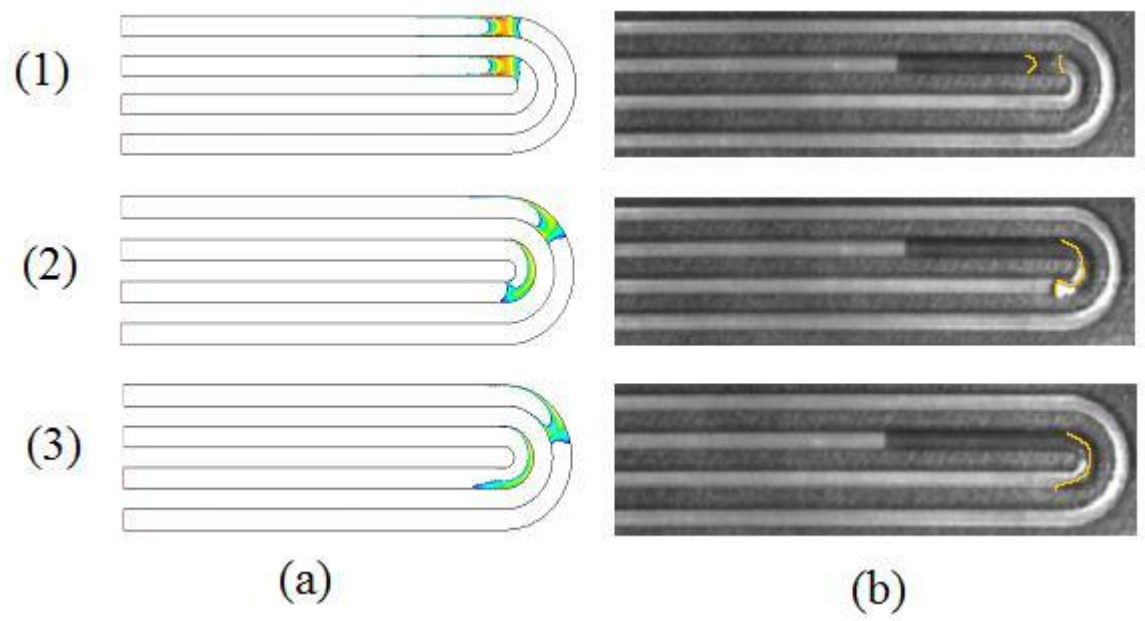

Figure 6 Results comparison (a) Model (volume fraction of water 0 to 0.9) (b) Experiment (1) 5.6 x10^{-3}sec (2) 8.2 x10^{-3}sec (3) 9 x10^{-3}sec.

4.2 Modelling & Experimental Results

In the following model images the channel walls are removed and planes are added for image clarity. The GDL is identified in images showing the volume fraction of water in the channels.

Scenario one investigates the movement of a single droplet into a second droplet that is positioned on the channel wall (outer channel) see Figure 7 (a). The single droplet, in the inner channel, is tracked to view any change that may be caused by the parallel channels and distribution of air in the channels. When both droplets join (in the outer channel) a large mass of water is produced, as shown in Figure 7 (b).

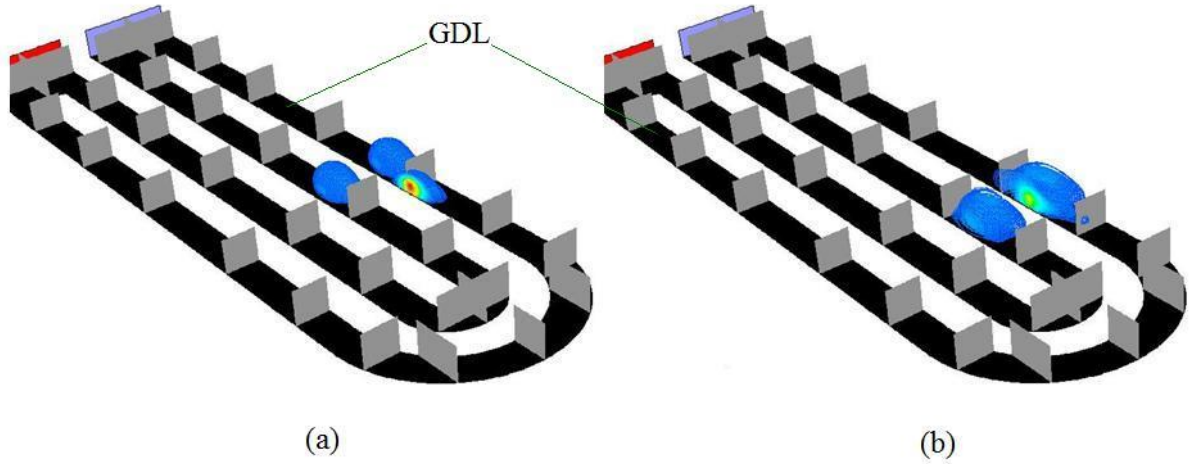

Figure 7 Droplets movement (Volume fraction of water 0 to 0.52) (a) Droplets move & join (Time step 400) (b) Slug forming (Time step 800).

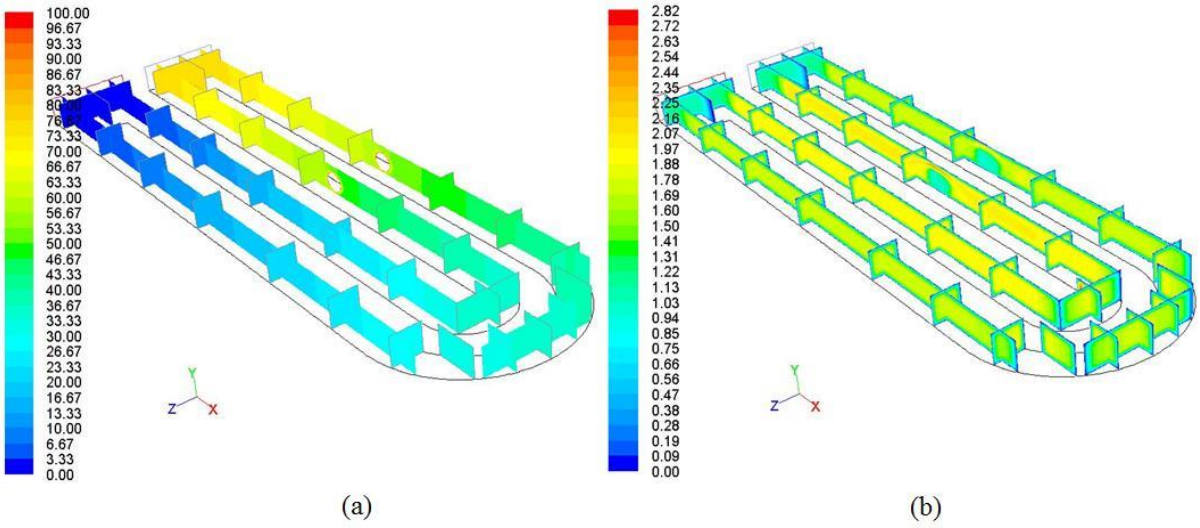

Figure 8 Droplets movement (a) Velocity (ms^{-1}) (b) Static pressure (pa) (Time step 40).

Contact: James.Carton3@mail.dcu.ie

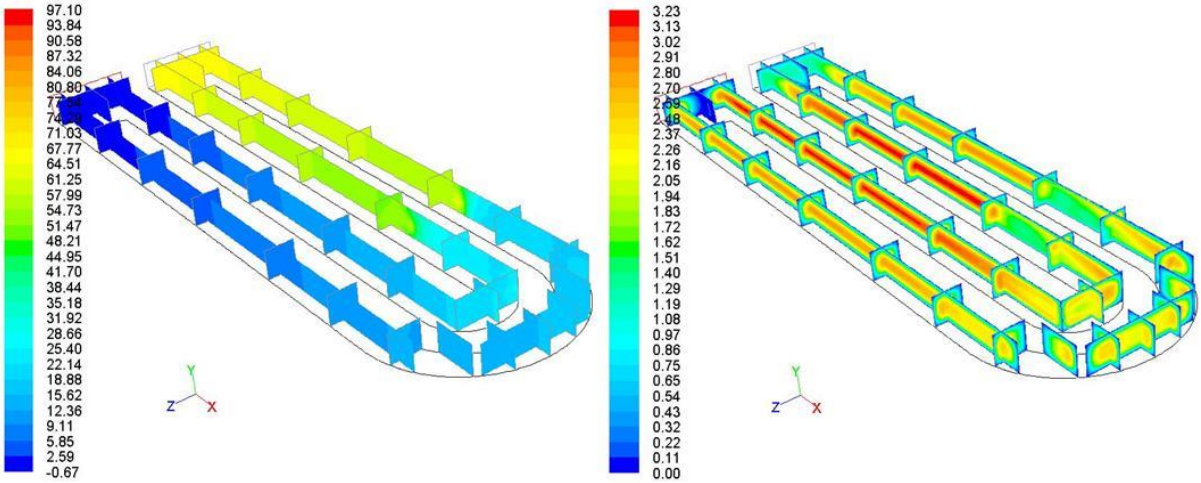

Figure 9 Droplets movement (a) Velocity (ms^{-1}) (b) Static pressure (pa) (Time step 800).

Time sequenced velocity and pressure results are shown in Figure 8 and Figure 9. At time step 40, velocity is observed to be in the range of 1.8 and 2ms^{-1} in both the inner and outer channels. There are velocity increases noticed around the droplets in the channels due to their restrictive affect in the channel. At time step 800, due to the interaction of the two droplets in the outer channel, the velocity increases in the inner channel, particularly noticeable over the droplet in this channel. Pressure also builds up when the droplets join, forming the slug and constricting airflow in the outer channel. When this occurs, low pressure is observed in the outer channel after the slug. Due to the mutual inlet channel region, the fluid in the out channel, which is blocked by the growing slug, uses the inner channel as a relief, increasing velocity and decreasing pressure across both channels. With increased velocity in the inner channel, pressure normalises as shown in Figure 9.

Scenario two investigates the movement of two droplets positioned on the outer channel wall. A single droplet, in the inner channel, is tracked to view any change that may be caused by the parallel channels and distribution of air in the channels. The single droplet (inner channel) moves quickly along the channel into the bend region due to its contact with the hydrophobic GDL. The two droplets in the outer channel move much slower due to their contact with the hydrophilic channel wall. As these droplets enter the bend region, they are seen to elongate due to the air interaction around the bend region.

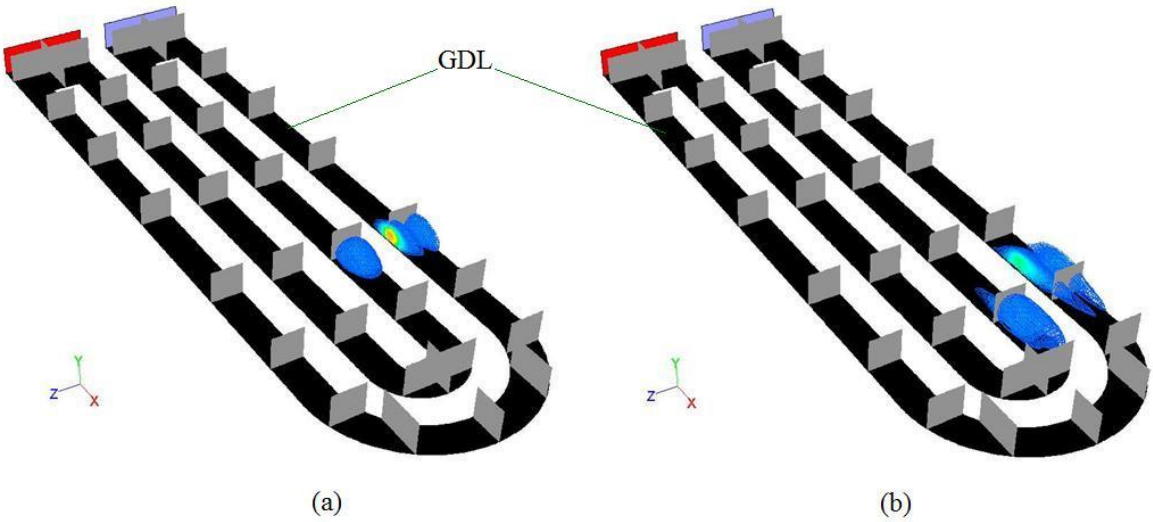

Figure 10 Droplets movement (Volume fraction of water 0 to 0.52) (a) Droplets move & join (Time step 400) (b) Slug forms but elongates (Time step 1000).

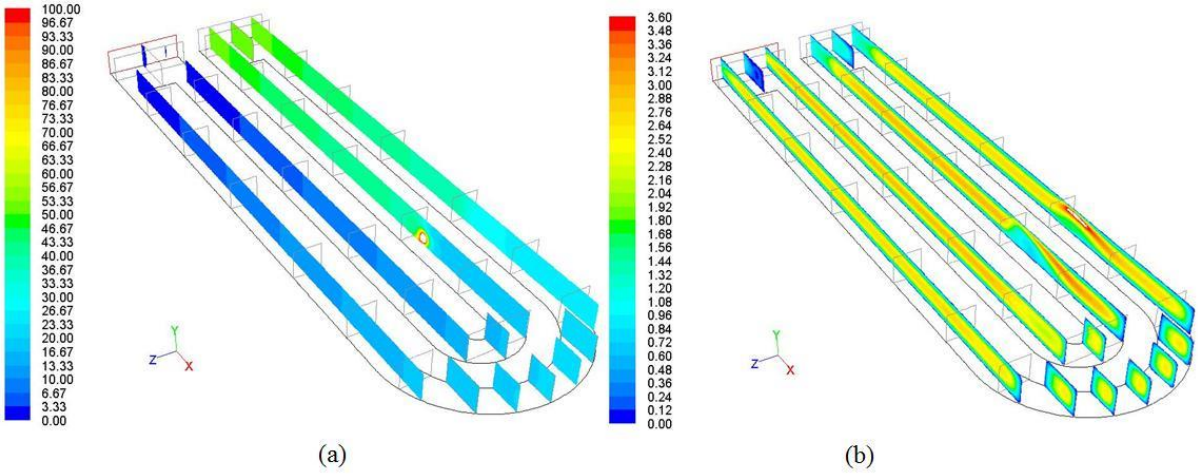

Figure 11 Droplets movement (a) Velocity (ms^{-1}) (b) Static pressure (pa) (Time step 400).

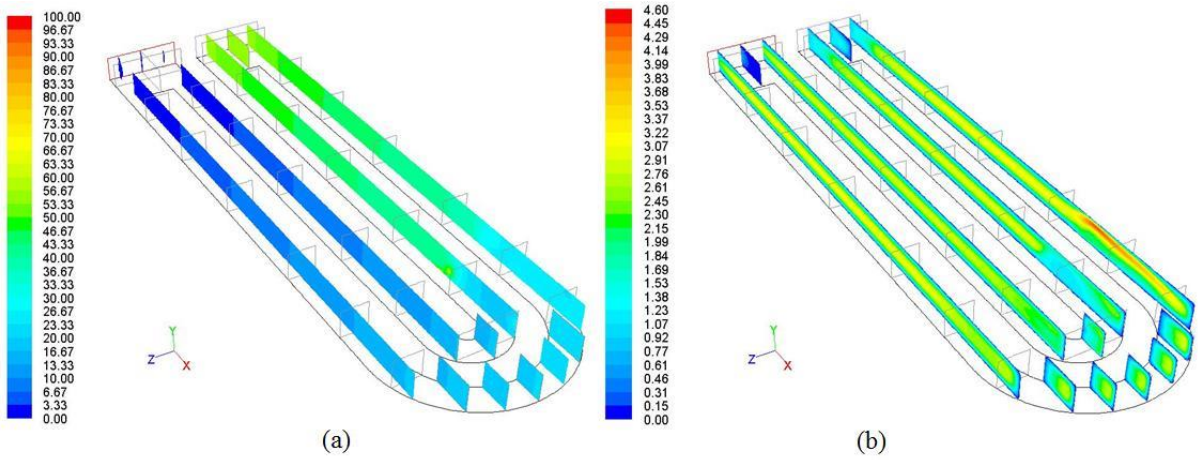

Figure 12 Droplets movement (a) Velocity (ms^{-1}) (b) Static pressure (pa) (Time step 800).

Contact: James.Carton3@mail.dcu.ie

The pressure and velocity analysis is shown in Figure 11 and Figure 12. The pressure is seen to be stable in all time steps showing that the droplets on the channel wall, in the outer channel, do not hinder the airflow. The droplets are disrupted by the faster airflow at the bend region and this may prove beneficial for water mitigation. The velocity is generally evenly distributed in the channels with highest velocity readings noticed around the droplets, in the outer channel before the bend region, due to their restrictive affect in the mini-channels.

Scenario three investigates the movement of a droplet into two droplets that are positioned on the channel wall (outer channel), see Figure 13 (a). A single droplet, in the inner channel, is tracked to view any change that may be caused by the parallel channels and distribution of air in the channels. The single droplet (inner channel) moves quickly along the channel due to its contact with the hydrophobic GDL. When droplets in the outer channel join a large mass of water is produced, almost blocking the air flow as shown in Figure 13 (b). The droplet in the inner channel is then seen to be pressed down to the GDL.

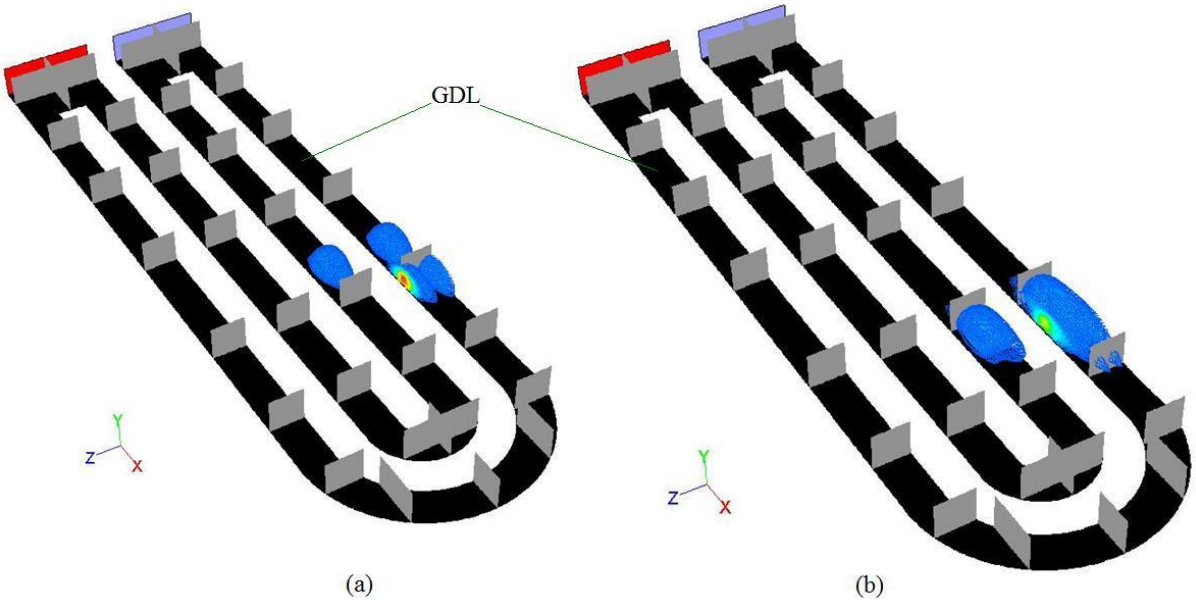

Figure 13 Droplets movement (Volume fraction of water 0 to 0.52) (a) Droplets move & join (Time step 400) (b) Slug forming (Time step 800)

Contact: James.Carton3@mail.dcu.ie

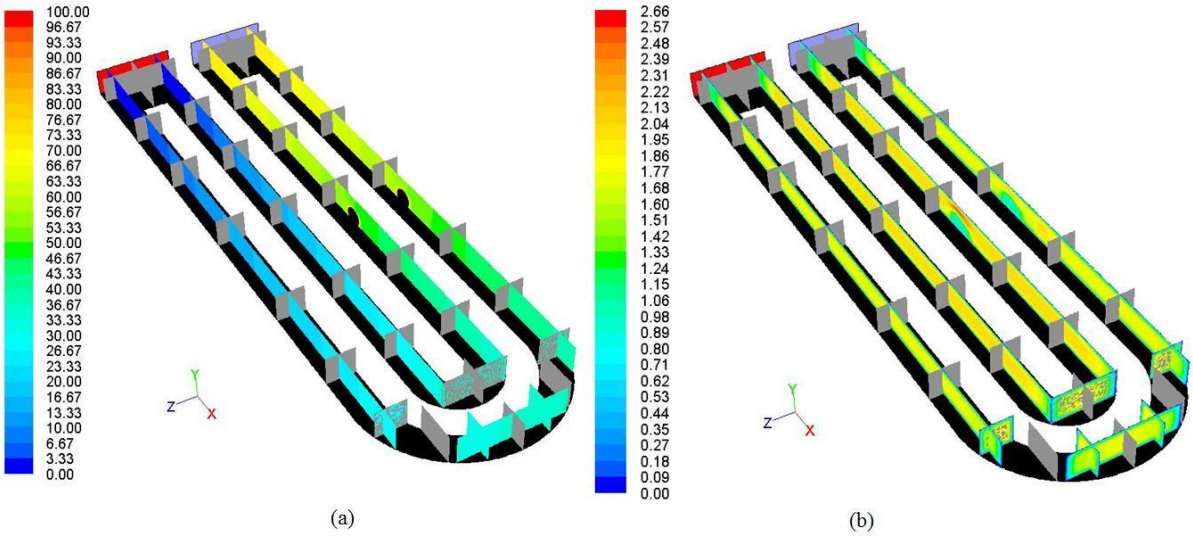

Figure 14 Droplets movement (a) Velocity (ms^{-1}) (b) Static pressure (pa) (Time step 40).

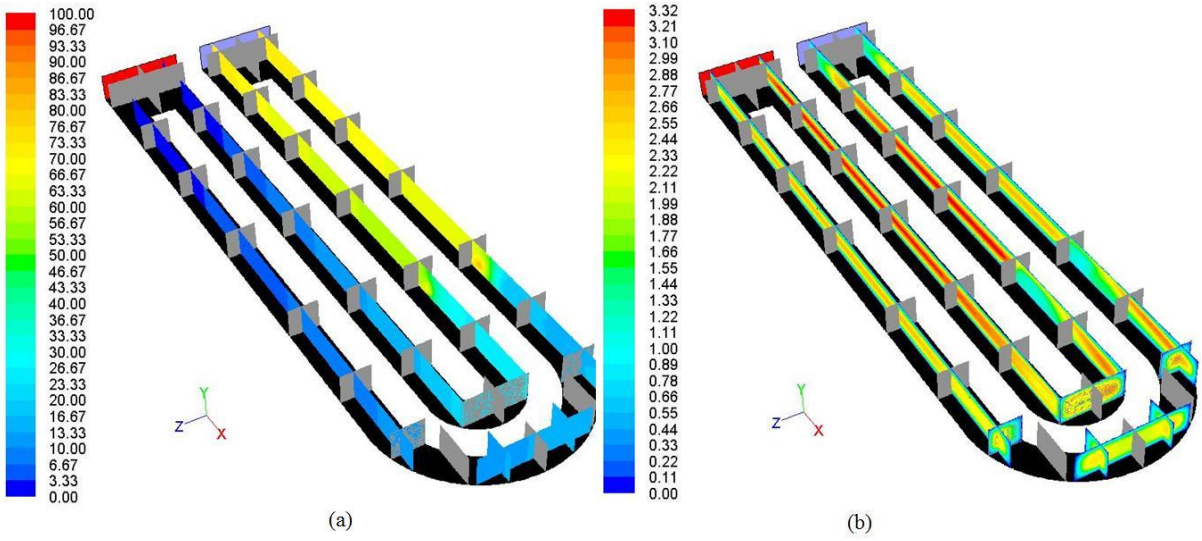

Figure 15 Droplets movement (a) Velocity (ms^{-1}) (b) Static pressure (pa) (Time step 800).

The time sequenced velocity and pressure analysis show the flow rate increases in the inner channel due to the slug (in the outer channel), constricting the flow, evident at time step 800 as shown in Figure 15. Due to the fast airflow, the droplet in the inner channel gets pushed to the surface of the GDL,. High velocity readings are noticed flowing over the water droplets, due to their restrictive affect in the mini-channels. The inner channel velocity reading is highest due to the blockage occurring in the outer channel.

The following simulation and experiment results show two straight mutual inlet channels each with a slug one bigger than the other. The air flow initially pushes both slugs down the channel, however

pressure builds up behind both slugs (up to 170 Pa) and the smaller slug starts to move faster. Figure 16 (2) shows the smaller slug moving past the larger slug. The pressure and velocity of the air then becomes large enough to burst the slug. This is visible in both the simulation and visualisation results. The pressure dramatically reduces to approximately 5 Pa in both channels increasing the flow rate of air in the smaller channel but the larger slug remains in the channel blocking it.

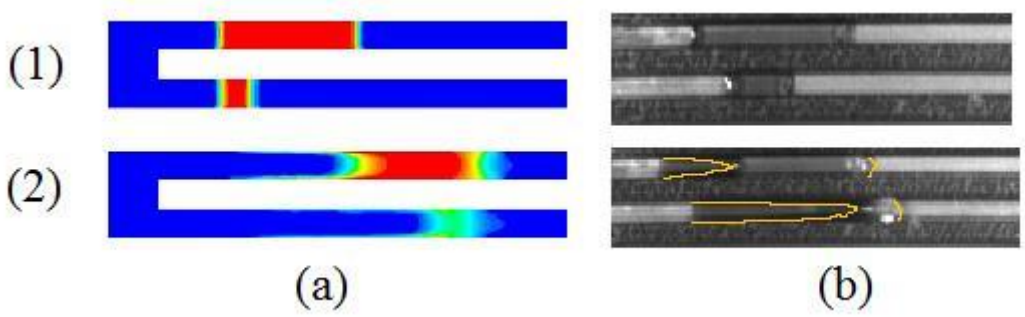

Figure 16 Results comparison (a) Model (volume fraction of water 0 to 0.9) (b) Experiment (1) Time step 40 (2) Time step 200

Figure 17 (a) shows a slug (red outline) approaching a stationary droplet (orange outline). Air flow escapes from around the stationary drop for the first three images. The characteristic movement of a slug is observed in Figure 17 (c), (d) & (e), due to the air flow around it. Once the slug comes close to the droplet, airflow becomes more restricted and this begins to deform and then move the previously stationary droplet as shown in Figure 17 (d) & (e). The slug however can quickly catch up on the droplet, they join and the droplet becomes larger.

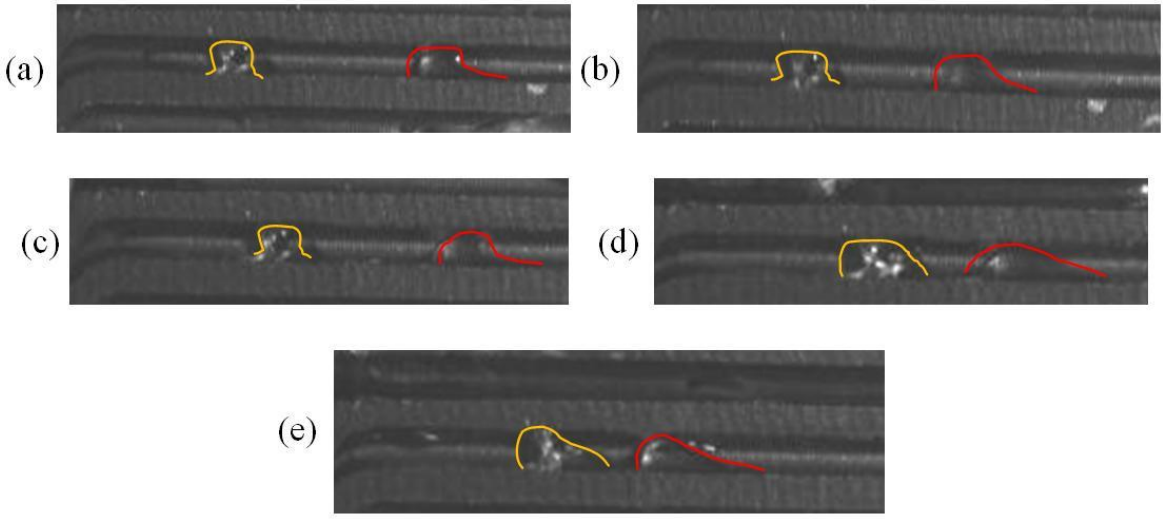

Figure 17 Slug & droplet interaction (a) 0sec (b) 16 x10^{-3}sec (c) 33 x10^{-3}sec (d) 50 x10^{-3}sec (e) 66 x10^{-3}sec

Contact: James.Carton3@mail.dcu.ie

5 DISCUSSION

If PEM fuel cells are operated below 100°C liquid water is produced in the cell. It is noted that if nafion based membranes continue to be used, good PEM fuel cell performance depends on good water management [44]. Water flooding in PEM fuel cells is a major issue and mitigation methods and/or techniques will ensure the full potential of these electrochemical devices.

The CFD VOF model was used in this study in order to investigate the interaction of the GDL and mini-channels with water flooding, specifically droplet coalescence as well as slug formation and movement within the mini-channels of a double serpentine PEM fuel cell. The 3-D double serpentine model layout with mutual inlet and outlet was used extensively with low flow rates. Lu et al. [37] employed an ex situ apparatus, to investigated the water transport in channels. They showed that at low flow rates ($1.7ms^{-1}$) slug flow dominated and these results matches well with this current study.

Hydrophobic and hydrophilic properties and the mini-channel design play a major role in the effective mitigation of flooding in flow plates. Spernjak et al. [45] investigated the effects of varying GDL materials and hydrophobicity. They found that PEM fuel cells with an untreated GDL was more prone to film and slug formation in the cathode gas channel. The present study used a hydrophobic GDL and it is found that slug flow dominated. The mini-channel walls had a lower contact angle than the GDL and hence the different contact angles affected the flow of water in the mini-channels, similar to findings by Du et al. [46].

When the channel walls are more hydrophobic (than the GDL), more water is accumulated on the GDL and this can dramatically affect voltage from the PEM fuel cell as shown by Ous and Arcoumanis [34]. Having the mini-channel walls less hydrophobic (than the GDL), causes any droplets produced by the cell to move to the channel walls, allowing the gas flow along the GDL as shown in Figure 10 (b). This can ensure that droplets can film flow along the channel walls, reducing their effect on mass transport through the GDL and interacting less with the pressure and flow in the channels as shown in Figure 11 and Figure 12 for example.

Once droplets coalesce a large droplet or slug can form in one channel and effectively block the channel, with low pressure observed in the blocked channel, after the blockage. This can reduce the PEM fuel cell's performance by almost 33%, also recognised by Hu et al. [47]. Due to mini-channel mutual inlets, the fluid in the blocked channel used the other, unblocked channel, as a relief, increasing velocity and decreasing pressure across both channels. With increased velocity, in the free channel, pressure can normalise, this was evident in the pressure and velocity results of Figure 9. If a second slug begins to form in the second channel, pressure can again build up forcing both slugs to move but most commonly the smaller slug will burst, as shown in Figure 16, sending micro droplets down the mini-channel. It is noticed that due to the bend areas in channels slugs become distorted and uneven pressures can effectively burst the largest slugs when carried into the bend region.

If these droplets are successfully moved from the cathode layer or GDL into the flow field, this does not ensure flood free fuel cell operation. Due to air flow and pressure gradients in the flow channels water droplets move, collide and grow within the flow channel flow path and consequently, liquid water flooding can occur downstream of the water source in the flow plate's flow fields. From this study the collision and coalescence of droplets can form slugs in PEM fuel cell mini-channels. A slug in a mini-channel can cause pressure drop oscillations and internal flow rate adjustment among the channels. Clogging of channels may occur when the slugs stagnate near a channel's exit region and completely stop gas flow through it. Smaller slugs may burst due to the pressure or flow rate. A slug has the potential to reducing the fuel cell performance.

6 CONCLUSIONS

In this study, using CFD modelling techniques a two-phase flow model was used to investigate the coalescence of droplets and movement of slugs in flow field mini-channels and with the aid of imaging techniques, visualisation of the water droplets and slugs were recorded in an ex situ apparatus. The implication of slugging on flow plate design and PEM fuel cell performance were discussed.

It is concluded that:

- Excess water in mini-channels from the collision and coalescence of droplets can directly form slugs in PEM fuel cells.
- Slugs can form at low flow rates (<5ms^{-1}) so increasing the flow rate in a PEM fuel cell can reduce the size and frequency of slugs.
- One channel of a double serpentine mini-channel (or similar parallel flow plate design) may become blocked due to the redistribution of air flow and pressure caused by slug formation.
- High pressure and velocity peaks observed during the formation of a slug could damage components such as the PEM fuel cell membrane.
- Correct GDL and mini-channel surface coatings are essential to reduce slug formation and stagnation.
- Voltage may be affected by the movement of slugs. By viewing constant voltage graphs of PEM fuel cells flooding may be detected.
- Having geometry changes (bends & steps) in the flow fields can disrupt slug movement and avoid channel blockages.

ACKNOWLEDGEMENT

The authors would like to thank the School of Engineering and Environmental Sciences in Wels Austria for use of their imaging devices.

REFERENCES

[1]Supramaniam S. Fuel Cells: From Fundamentals to Applications New York: Springer Science & business Media; 2006, ISBN 0-387-25116-2.

[2]Lawlor V, Zauner G, Hochenauer C, Mariani A, Griesser S, Carton JG, et al. The Use of a High Temperature Wind Tunnel for MT-SOFC Testing-Part I: Detailed Experimental Temperature Measurement of an MT-SOFC Using an Avant-Garde High Temperature Wind Tunnel and Various Measurement Techniques. Journal of Fuel Cell Science and Technology 2010 12;7(6):061016 (7 pp.).

[3]Carton JG, Olabi AG. Wind/hydrogen hybrid systems: Opportunity for Ireland's wind resource to provide consistent sustainable energy supply. Energy 2010;35(12):4536-4544.

[4]H. R. Haas and M. T. Davis. Electrode and catalyst durability requirements in automotive PEM applications: Technology status of a recent MEA design and next generation challenges. Anonymous

9th Proton Exchange Membrane Fuel Cell Symposium (PEMFC 9) - 216th Meeting of the Electrochemical Society, October 4, 2009 - October 925 Vienna, Austria: Electrochemical Society Inc; 2009; 1623-1631.

[5]Achour H, Carton JG, Olabi AG. Estimating vehicle emissions from road transport, case study: Dublin City. 2011.

[6]Neef H-. International overview of hydrogen and fuel cell research. Energy 2009 03;34(3):327-33.

[7]Hassan NSM, Daud WRW, Sopian K, Sahari J. Water management in a single cell proton exchange membrane fuel cells with a serpentine flow field. J.Power Sources 2009;193(1):249-257.

[8]Pasaogullari U, Wang CY. Liquid water transport in gas diffusion Layer of polymer electrolyte fuel cells. J.Electrochem.Soc. 2004 03;151(3):399-406.

[9]J. S. Yi and T. V. Nguyen. The effect of the flow distributor on the performance of PEM fuel cells. Anonymous Proceeding of the First International Symposium on Proton Conducting Membrane Fuel Cells 1 Pennington, NJ, USA: Electrochem. Soc; 8 Oct. 1995; 66-75.

[10]Li X, Sabir I, Park J. A flow channel design procedure for PEM fuel cells with effective water removal. J.Power Sources 2007 01/01;163(2):933-42.

[11]Jin HN, Kyu-Jin Lee, Gi-Suk Hwang, Charn-Jung Kim, Kaviany M. Microporous layer for water morphology control in PEMFC. Int.J.Heat Mass Transfer 2009 05;52(11-12):2779-91.

[12]Jin HN, Kaviany M. Effective diffusivity and water-saturation distribution in single- and two-layer PEMFC diffusion medium. Int.J.Heat Mass Transfer 2003 11;46(24):4595-611.

[13]Djilali N, Litster S, Sinton D. Ex situ visualization of liquid water transport in PEM fuel cell gas diffusion layers. J.Power Sources 2006 03/09;154(1):95-105.

[14]Holmstrom N, Ihonen J, Lundblad A, Lindbergh G. The influence of the gas diffusion layer on water management in polymer electrolyte fuel cells. Fuel Cells 2007;7(4):306-13.

[15]Xiao-Dong Wang, Yuan-Yuan Duan, Wei-Mon Yan, Xiao-Feng Peng. Local transport phenomena and cell performance of PEM fuel cells with various serpentine flow field designs. J.Power Sources 2008 01/03;175(1):397-407.

[16]Wills J. Imaging water in PEM fuel cells. Fuel Cell Review 2005;2(5):27-29.

[17]Xiao-Dong Wang, Xin-Xin Zhang, Wei-Mon Yan, Duu-Jong Lee, Su A. Determination of the optimal active area for proton exchange membrane fuel cells with parallel, interdigitated or serpentine designs. Int J Hydrogen Energy 2009 05;34(9):3823-32.

[18]Djilali N. Computational modelling of polymer electrolyte membrane (PEM) fuel cells: Challenges and opportunities. Energy 2007 04;32(4):269-80.

Contact: James.Carton3@mail.dcu.ie

[19]Siegel C. Review of computational heat and mass transfer modeling in polymer-electrolyte-membrane (PEM) fuel cells. Energy 2008;33(9):1331-1352.

[20]Kumbur EC, Sharp KV, Mench MM. Liquid droplet behavior and instability in a polymer electrolyte fuel cell flow channel. J.Power Sources 2006 10/20;161(1):333-345.

[21]Park J, Li X. Multi-phase micro-scale flow simulation in the electrodes of a PEM fuel cell by lattice Boltzmann method. J.Power Sources 2008 03/15;178(1):248-57.

[22]Erin Kimball, Tamara Whitaker, I. G. Kevrekidis and J. B. Benziger. Drops, slugs and flooding in PEM fuel cells. Anonymous 7th Symposium Devoted to Proton Exchange Membrane Fuel Cells - 212th ECS Meeting, October 7, 2007 - October 1211 Washington, DC, United states: Electrochemical Society Inc; 2007; 725-736.

[23]Yang XG, Zhang FY, Lubawy AL, Wang CY. Visualization of liquid water transport in a PEFC. Electrochemical and Solid-State Letters 2004 11;7(11):408-11.

[24]Hakenjos A, Muenter H, Wittstadt U, Hebling C. A PEM fuel cell for combined measurement of current and temperature distribution, and flow field flooding. J.Power Sources 2004;131(1-2):213-216.

[25]Gao B, Steenhuis TS, Zevi Y, Parlange J-, Carter RN, Trabold TA. Visualization of unstable water flow in a fuel cell gas diffusion layer. J.Power Sources 2009;190(2):493-498.

[26]Zhu X, Sui PC, Djilali N. Dynamic behaviour of liquid water emerging from a GDL pore into a PEMFC gas flow channel. J.Power Sources 2007;172(1):287-295.

[27]Tüber K, Pócza D, Hebling C. Visualization of water buildup in the cathode of a transparent PEM fuel cell. J.Power Sources 2003 11/24;124(2):403-414.

[28]Ge S, Chao-Yang Wang. Liquid water formation and transport in the PEFC anode. J.Electrochem.Soc. 2007 10;154(10):B998-B1005.

[29]Quan P, Ming-Chia Lai. Numerical study of water management in the air flow channel of a PEM fuel cell cathode. J.Power Sources 2007 01/10;164(1):222-37.

[30]Liu Z, Mao Z, Wang C. A two dimensional partial flooding model for PEMFC. J.Power Sources 2006 8/25;158(2):1229-1239.

[31]Zhu X, Liao Q, Sui PC, Djilali N. Numerical investigation of water droplet dynamics in a low-temperature fuel cell microchannel: effect of channel geometry. J.Power Sources 2010 02/01;195(3):801-12.

[32]Carton JG, Olabi AG. Design of experiment study of the parameters that affect performance of three flow plate configurations of a proton exchange membrane fuel cell. Energy 2010;35(7):2796-2806.

Contact: James.Carton3@mail.dcu.ie

[33]Li H, Tang Y, Wang Z, Shi Z, Wu S, Song D, et al. A review of water flooding issues in the proton exchange membrane fuel cell. J.Power Sources 2008 03/15;178(1):103-17.

[34]Ous T, Arcoumanis C. Visualisation of water droplets during the operation of PEM fuel cells. J.Power Sources 2007 11/08;173(1):137-48.

[35]Weng F, Su A, Hsu C, Lee C. Study of water-flooding behaviour in cathode channel of a transparent proton-exchange membrane fuel cell. J.Power Sources 2006 7/3;157(2):674-680.

[36]Hussaini IS, Wang C. Visualization and quantification of cathode channel flooding in PEM fuel cells. J.Power Sources 2009;187(2):444-451.

[37]Lu Z, Kandlikar SG, Rath C, Grimm M, Domigan W, White AD, et al. Water management studies in PEM fuel cells, Part II: ex situ investigation of flow maldistribution, pressure drop and two-phase flow pattern in gas channels. Int J Hydrogen Energy 2009 05;34(8):3445-56.

[38]Zhou B, Quan P, Sobiesiak A, Liu Z. Water behavior in serpentine micro-channel for proton exchange membrane fuel cell cathode. J.Power Sources 2005 12/01;152:131-45.

[39]Fluent Inc. Fluent Manual & Tutorials. U.S.,See Also: http://my.fit.edu/itresources/manuals/fluent6.3/help/, Accessed 2010.

[40]Van SA, Deen NG, Kuipers JAM. Numerical simulation of gas bubbles behaviour using a three-dimensional volume of fluid method. Chemical Engineering Science 2005;60(11):2999-3011.

[41]F. Lai, C. Sanchez and M. Sanchez. Numerical Simulation of Thermocapillary Pumping Using the Volume of Fluid Method. Anonymous Oklahoma Science86 Oklahoma; 2006; 75-83.

[42]Theodorakakos A, Ous T, Gavaises M, Nouri JM, Nikolopoulos N, Yanagihara H. Dynamics of water droplets detached from porous surfaces of relevance to PEM fuel cells. J.Colloid Interface Sci. 2006;300(2):673-687.

[43]Bazylak A, Heinrich J, Djilali N, Sinton D. Liquid water transport between graphite paper and a solid surface. J.Power Sources 2008;185(2):1147-1153.

[44]Curtin DE, Lousenberg RD, Henry TJ, Tangeman PC, Tisack ME. Advanced materials for improved PEMFC performance and life. J.Power Sources 2004;131(1-2):41-48.

[45]Advani SG, Spernjak D, Prasad AK. Experimental investigation of liquid water formation and transport in a transparent single-serpentine PEM fuel cell. J.Power Sources 2007 07/10;170(2):334-44.

[46]Du W, Zhang L, Bi XT, Wilkinson D, Stumper J, Wang H. Two-dimensional simulations of gas-liquid two-phase flow in mini channels of PEM fuel cell flow field. International Journal of Chemical Reactor Engineering 2010;8.

[47]Hu M, Zhu X, Gu A. Simulation of the internal transport phenomena for PEM fuel cells with different modes of flow. Chin.J.Chem.Eng. 2004;12(1):14-26.

Contact: James.Carton3@mail.dcu.ie